

Two-body density matrix for closed $s - d$ shell nuclei

S.S. Dimitrova, D.N. Kadrev, A.N. Antonov, M.V. Stoitsov

Institute of Nuclear Research and Nuclear Energy, Bulgarian, Academy of Sciences, Sofia 1784, Bulgaria

Received: 11 September 1999 / Revised version: 20 December 1999

Communicated by P. Schuck

Abstract. The two-body density matrix for ${}^4\text{He}$, ${}^{16}\text{O}$ and ${}^{40}\text{Ca}$ within the Low-order approximation of the Jastrow correlation method is considered. Closed analytical expressions for the two-body density matrix, the center of mass and relative local densities and momentum distributions are presented. The effects of the short-range correlations on the two-body nuclear characteristics are investigated.

PACS. 21.60.-n Nuclear-structure models and methods

1 Introduction

Nowadays two-body knock-out reactions such as (γ, NN) [1,2] and $(e, e'NN)$ [3–6] are intensively studied in order to extract information about the nucleon-nucleon short-range correlations (SRC) in nuclei. In particular, the cross section for the two-nucleon emission processes is generally related to the two-body spectral function at least in PWIA [7]. The two-body currents and the final state interactions should be also taken into account. The first calculations of the two-nucleon spectral function of ${}^{16}\text{O}$ have already been performed [8] by treating the long-range correlations within a Dressed RPA approach and including the SRC in terms of the defect functions emerging as a solution of the Bethe–Goldstone equation for finite nuclei. The results have been successfully applied for calculating the $(e, e'pp)$ cross-sections [6].

Due to the complexity of the problem, however, it is highly desirable to reach a theoretical description of the two-body knock-out reactions directly in terms of the nuclear ground state (e.g., the ground-state two-body density matrix) without the necessity to deal with the two-body spectral function which is an enormously more complicated object due to the presence of various excited states of the system. Making use of series of more or less controlled approximations, people usually try to incorporate in this context simplified expressions or combinations of physical quantities such as the two-particle spectroscopic factors and overlap functions [9], relative and center-of-mass pair momentum distributions, combined two-body momentum distributions [10] and generalized momentum distributions (see e.g. [11]).

The situation is quite similar to the theoretical description of one-particle removal processes in terms of the nuclear ground state characteristics. At the beginning, it has been demonstrated [16] that the knowledge of the ground-

state one-body density matrix of the target nucleus is sufficient to restore the single-particle overlap functions, spectroscopic factors and separation energies associated with the bound $(A - 1)$ -particle eigenstates. Then, quantitative estimates have been obtained [17] within a simple and analytical one-body density matrix model [18] which takes into account the short-range correlations in terms of the Jastrow correlation method. Plausible conclusions have been made for the properties of single-particle overlap functions in comparison with the associated shell model orbitals and the natural orbitals [18–20] which are of frequent interest in this context [21,22]. The resulting overlap functions and spectroscopic factors have been used to analyze differential cross sections of (p, d) reactions and single-particle momentum distributions in $(e, e'p)$ reactions [23]. Finally, more sophisticated representations of the one-body density matrix [24–26] have been used for extracting overlap functions and spectroscopic factors further applied for analyzing (p, d) reaction cross-sections [27]. Thus, the resulting comparative study [27] has clarified the impact of the different types of nucleon-nucleon correlations on the one-particle removal reaction cross-sections.

Recently, similar restoration procedure has been proposed in [28] connecting the two-nucleon overlap functions associated with the bound states of the $(A - 2)$ - or $(A - 2)$ -particle system with the asymptotic behavior of the ground state two-body density matrix of the A -particle system. This makes it possible to calculate, at least in principle, the two-body overlap functions, spectroscopic factors and separation energies on the basis of realistic representations for the ground state two-body density matrix.

To test the restoration procedure for the two-nucleon overlap functions one clearly needs a simple and analytical representation of the two-body density matrix which adequately reflects the properties of the nuclear ground state

and also takes into account the short-range correlations in nuclei.

The present paper suggests such a simple and analytical representation of the ground state two-body density matrix derived within the Low-order approximation of the Jastrow correlation method. The associated two-particle nuclear characteristics for the closed $s - d$ shell nuclei ${}^4\text{He}$, ${}^{16}\text{O}$ and ${}^{40}\text{Ca}$ are analyzed. A comparison with the realistic Variational Monte-Carlo calculations [12–14] is also made. It justifies the physical meaning of the approximation as a tool for analyzing the impact of the nuclear SRC in a simple way. The analytical expressions obtained can facilitate the explanation of questions arising from the interpretation of physical properties which are important in treating the two-particle emission processes in nuclei.

The paper is organized as follows. The general definitions of the two-body density matrix and the associated nuclear characteristics in coordinate and momentum representation are introduced in Sect. 2. The analytical expressions derived within the Low-order approximation of the Jastrow correlation method are given in Sect. 3. Closed analytical expressions for the two-body nucleon momentum and density distributions are collected in Sect. 4. Results and discussions are given in Sect. 5, while the conclusions are summarized in Sect. 6. The Appendix contains the coefficients entering the analytical expressions for ${}^4\text{He}$ and ${}^{16}\text{O}$ nuclei.

2 Two-body density matrix

2.1 Definitions and properties

The physical antisymmetric state of a system of A identical fermions Ψ^A normalized to unity defines a set of density matrices of order $p = 1, 2, \dots, A$

$$\rho^{(p)}(x_1, x_2, \dots, x_p; x'_1, x'_2, \dots, x'_p) = \langle \Psi | a^\dagger(x_1) a^\dagger(x_2) \dots a^\dagger(x_p) a(x'_1) a(x'_2) \dots a(x'_p) | \Psi \rangle, \quad (1)$$

where $a^\dagger(x_i)$ and $a(x_i)$ stand for creation and annihilation operators for a nucleon at position x_i , which includes the spatial coordinate \mathbf{r}_i , the spin s_i and the isospin τ_i . In particular, the one- and two-body density matrices are defined in coordinate space as:

$$\rho^{(1)}(x, x') = \langle \Psi^{(A)} | a^\dagger(x) a(x') | \Psi^{(A)} \rangle, \quad (2)$$

and

$$\rho^{(2)}(x_1, x_2; x'_1, x'_2) = \langle \Psi^{(A)} | a^\dagger(x_1) a^\dagger(x_2) a(x'_1) a(x'_2) | \Psi^{(A)} \rangle, \quad (3)$$

respectively. From these defining equations one can easily recognize many of the properties of the density matrices. They are Hermitian

$$\begin{aligned} \rho^{(1)}(x, x') &\equiv \rho^{(1)*}(x'; x), \\ \rho^{(2)}(x_1, x_2; x'_1, x'_2) &= \rho^{(2)*}(x'_1, x'_2; x_1, x_2), \end{aligned} \quad (4)$$

and trace-normalized to the number of particles and of pairs of particles:

$$\text{Tr} \rho^{(1)} = \int \rho(x) dx = A, \quad (5)$$

$$\text{Tr} \rho^{(2)} = \frac{1}{2} \int \rho^{(2)}(x_1, x_2) dx_1 dx_2 = \frac{A(A-1)}{2}, \quad (6)$$

with diagonal symmetric elements

$$\rho(x) = \rho^{(1)}(x, x), \quad \rho^{(2)}(x_1, x_2) = \rho^{(2)}(x_1 x_2; x_1 x_2). \quad (7)$$

In addition, the two-body density matrix $\rho^{(2)}$ is antisymmetric in each set of indices, e.g.,

$$\rho^{(2)}(x_1 x_2; x'_1 x'_2) = -\rho^{(2)}(x_2 x_1; x'_1 x'_2), \quad (8)$$

so that its diagonal elements vanish identically if both coordinates are equal, i.e., $\rho^{(2)}(x_1, x_1) = 0$.

The one- and two-body density matrices are related by the formula

$$\int \rho^{(2)}(x_1 x_2; x'_1 x'_2) dx_2 = \frac{A-1}{2} \rho^{(1)}(x_1, x'_1), \quad (9)$$

and both can be presented in the momentum space using the Fourier transforms:

$$n^{(1)}(k; k') = \int \rho(x, x') \exp[i(\mathbf{k} \cdot \mathbf{r} - \mathbf{k}' \cdot \mathbf{r}')] d\mathbf{r} d\mathbf{r}' \quad (10)$$

$$\begin{aligned} n^{(2)}(k_1, k_2; k'_1, k'_2) &= \int \rho^{(2)}(x_1, x_2; x'_1, x'_2) \\ &\times \exp[i(\mathbf{k}_1 \cdot \mathbf{r}_1 + \mathbf{k}_2 \cdot \mathbf{r}_2 - \mathbf{k}'_1 \cdot \mathbf{r}'_1 - \mathbf{k}'_2 \cdot \mathbf{r}'_2)] \\ &\times d\mathbf{r}_1 d\mathbf{r}_2 d\mathbf{r}'_1 d\mathbf{r}'_2, \end{aligned} \quad (11)$$

where k_i stands for the momentum \mathbf{k}_i , spin s_i and isospin τ_i of the i -th particle. Relations similar to (4)–(8) held for the one- and two-body density matrices in the momentum space as well.

2.2 Two-body nuclear characteristics

Typical ground state quantities of interest one usually considers are the local density

$$\rho(\mathbf{r}) \equiv \rho(\mathbf{r}, \mathbf{r}) = \sum_{s\tau} \rho(x, x), \quad (12)$$

the associated elastic form-factor

$$F(\mathbf{q}) = \frac{1}{A} \int \rho(\mathbf{r}) \exp[i\mathbf{q} \cdot \mathbf{r}] d\mathbf{r} \quad (13)$$

and the nucleon momentum distribution

$$n(\mathbf{k}) \equiv n(\mathbf{k}, \mathbf{k}) = \sum_{s\tau} n(k, k) \quad (14)$$

obtained after spin (and/or isospin) summation of the diagonal elements of the one-body density matrix in coordinate and momentum representation.

The two-particle emission experiments however require some knowledge of physical quantities associated with the two-body density matrix. For example, the diagonal elements of the two-body density matrix $\rho^{(2)}$ in coordinate space, (3), define the center-of-mass pair local density distribution:

$$\rho^{(2)}(\mathbf{R}) = \int \rho^{(2)}(\mathbf{R} + \mathbf{s}/2, \mathbf{R} - \mathbf{s}/2) d\mathbf{s} \quad (15)$$

and the relative local density distribution:

$$\rho^{(2)}(\mathbf{s}) = \int \rho^{(2)}(\mathbf{R} + \mathbf{s}/2, \mathbf{R} - \mathbf{s}/2) d\mathbf{R} \quad (16)$$

while the diagonal elements in momentum space (11) define the associated center-of-mass and relative pair momentum distributions:

$$n^{(2)}(\mathbf{K}) = \int n^{(2)}(\mathbf{K}/2 + \mathbf{k}, \mathbf{K}/2 - \mathbf{k}) d\mathbf{k} \quad (17)$$

and

$$n^{(2)}(\mathbf{k}) = \int n^{(2)}(\mathbf{K}/2 + \mathbf{k}, \mathbf{K}/2 - \mathbf{k}) d\mathbf{K}, \quad (18)$$

respectively.

The physical meaning of $\rho^{(2)}(\mathbf{s})$ and $n^{(2)}(\mathbf{k})$ is the probability to find two particles displaced of a certain relative distance $\mathbf{s} = \mathbf{r}_1 - \mathbf{r}_2$ or moving with relative momentum $\mathbf{k} = (\mathbf{k}_1 - \mathbf{k}_2)/2$, respectively, while $\rho^{(2)}(\mathbf{R})$ and $n^{(2)}(\mathbf{K})$ represents the probability to find a pair of particles with center-of-mass coordinate $\mathbf{R} = (\mathbf{r}_1 + \mathbf{r}_2)/2$ or center-of-mass momentum $\mathbf{K} = \mathbf{k}_1 + \mathbf{k}_2$, respectively.

3 Analytical expressions for the two-body density matrix

3.1 Mean-field approximation

The mean-field approximation to the nuclear ground state of an A particle system is represented by a single Slater determinant

$$\Phi_{SD}^A(x_1, x_2, \dots, x_A) = \frac{1}{\sqrt{A!}} \det |\varphi_i(x_j)|, \quad (19)$$

where the orthonormalized set of single-particle functions $\varphi_i(x) = \varphi_i(\mathbf{r}, s, \tau)$ is emerging from some kind of shell model or self-consistent mean-field calculations. The ground state Φ_{SD}^A incorporates two kinds of correlations: (1) Pauli correlations associated with the antisymmetric properties of Φ_{SD}^A and (2) the correlations among the nucleons forming the nuclear mean field that determines the particular form of the single particle states $\varphi_i(x)$.

The following expressions for the one- and two-body density matrices are well known from the mean-field theory

$$\rho_{SD}(x, x') = \sum_{i=1}^A \varphi_i^*(x) \varphi_i(x'), \quad (20)$$

$$\rho_{SD}^{(2)}(x_1 x_2; x'_1 x'_2) = \sum_{i,j=1}^A \varphi_{ij}^*(x_1 x_2) \varphi_{ij}(x'_1 x'_2), \quad (21)$$

where the antisymmetric uncorrelated two-body wave functions are used

$$\varphi_{ij}(x_1 x_2) = \frac{1}{\sqrt{2}} [\varphi_i^*(x_1) \varphi_j(x_2) - \varphi_j^*(x_1) \varphi_i(x_2)]. \quad (22)$$

In order to obtain analytical expressions which will allow us to compute ρ_{SD} and $\rho_{SD}^{(2)}$ in a direct way we further assume all states belonging to the uncorrelated Fermi sea as represented by harmonic oscillator single-particle wave functions $\varphi_i^{HO}(x)$ which depend on the harmonic oscillator length α , having the same values for protons and neutrons. In particular, these are the states $1s$ for 4He , $1s$ and $1p$ for ${}^{16}O$ and $1s, 1p, 1d$ and $2s$ for ${}^{40}Ca$. Because we are interested in spin (and/or isospin) free quantities like total center of mass and relative coordinate and momentum distributions we consider only the matrix elements which are fully diagonal in spin and isospin variables. Under these assumptions (21) has closed analytical form:

$$\begin{aligned} \rho_{SD}^{(2)}(\mathbf{r}_1, s_1, \tau_1; \mathbf{r}_2, s_2, \tau_2; \mathbf{r}_3, s_1, \tau_1; \mathbf{r}_4, s_2, \tau_2) \\ = \frac{1}{2} [\rho(\mathbf{r}_1, \mathbf{r}_3) \rho(\mathbf{r}_2, \mathbf{r}_4) - \delta_{\tau_1 \tau_2} \delta_{s_1 s_2} \rho(\mathbf{r}_1, \mathbf{r}_4) \rho(\mathbf{r}_2, \mathbf{r}_3)], \end{aligned} \quad (23)$$

since the spin and isospin free one-body density matrix

$$\rho(\mathbf{r}_1, \mathbf{r}_2) = \sum_{s\tau} \rho_{SD}(\mathbf{r}_1, s, \tau; \mathbf{r}_2, s, \tau) \quad (24)$$

is an explicit product of exponent and polynomial factors depending only on the scaled coordinates $\mathbf{x}_i = \alpha \mathbf{r}_i$:

$$\rho(\mathbf{r}_1, \mathbf{r}_2) = \frac{\alpha^3}{\pi^{3/2}} \exp\left[-\frac{\mathbf{x}_1^2 + \mathbf{x}_2^2}{2}\right] P_{SD}(\mathbf{x}_1, \mathbf{x}_2), \quad (25)$$

where

$$\begin{aligned} P_{SD}(\mathbf{x}_1, \mathbf{x}_2) &= 1 && \text{for } {}^4He, \\ &= (1 + 2x_{12}) && \text{for } {}^{16}O, \\ &= \frac{1}{2} [5 + 4x_{12} - 2(x_1^2 - 2x_{12} + x_2^2)] && \text{for } {}^{40}Ca \end{aligned} \quad (26)$$

and $x_{ij} \equiv \mathbf{x}_i \cdot \mathbf{x}_j = \alpha^2 r_i r_j \cos \theta_{ij}$, θ_{ij} being the angle between radius vectors \mathbf{r}_i and \mathbf{r}_j .

3.2 Jastrow correlations method

In the present paper we consider the nucleon-nucleon SRC within the Jastrow correlation method [29–32]. This method incorporates the nucleon-nucleon SRC in terms of the wave function ansatz:

$$\begin{aligned} \Psi^{(A)}(\mathbf{r}_1, \mathbf{r}_2, \dots, \mathbf{r}_A) &= (C_A)^{-1/2} \prod_{1 \leq i < j \leq A} f(|\mathbf{r}_i - \mathbf{r}_j|) \\ &\quad \times \Phi_{SD}^A(\mathbf{r}_1, \mathbf{r}_2, \dots, \mathbf{r}_A), \end{aligned} \quad (27)$$

where Φ_{SD}^A is a single Slater determinant, $f(\mathbf{r})$ is a correlation factor which goes to unity for large values of \mathbf{r} and C_A is a normalization constant. Except for systems containing very small number of particles it is impossible to calculate the one- and two-body density matrices using the Jastrow ansatz (27). One usually applies a perturbation expansion in terms of linked diagrams [30]. The so-called Low-order approximation (LOA) keeps all terms up to second order in $h = f - 1$ and first order in $g = f^2 - 1$ in such a way that the normalization of the density matrices is ensured order by order [30]. In particular, the resulting two-body density matrix is of the form [31, 32]:

$$\begin{aligned} \rho_{LOA}^{(2)}(x_1, x_2; x_3, x_4) &= \\ \rho_{SD}^{(2)}(1234) &+ [f_{13}^* f_{24} - 1] \rho_{SD}^{(2)}(1234) \\ &+ \int dx_5 [(f_{15}^* f_{35} - 1) + (f_{25}^* f_{45} - 1)] \\ \times [\rho_{SD}(x_1; x_3) \rho_{SD}^{(2)}(2545) &+ \rho_{SD}(x_1; x_4) \rho_{SD}^{(2)}(2553) \\ &+ \rho_{SD}(x_1; x_5) \rho_{SD}^{(2)}(2534)] \\ &+ \int \int dx_5 dx_6 [f_{56}^* f_{56} - 1] \left\{ \rho_{SD}^{(2)}(2665) \rho_{SD}^{(2)}(1534) \right. \\ &+ \rho_{SD}(x_1; x_5) \rho_{SD}(x_2; x_3) \rho_{SD}^{(2)}(5646) \\ &+ \rho_{SD}(x_1; x_5) \rho_{SD}(x_2; x_4) \rho_{SD}^{(2)}(5663) \\ &\left. + \rho_{SD}(x_1; x_5) \rho_{SD}(x_2; x_6) \rho_{SD}^{(2)}(5634) \right\}, \end{aligned} \quad (28)$$

where $f_{ij} \equiv f(|\mathbf{r}_i - \mathbf{r}_j|)$, $\rho_{SD}^{(2)}(1234) \equiv \rho_{SD}^{(2)}(x_1, x_2; x_3, x_4)$ and the integration over x_i means summation over the spin and isospin variables and integration over the spacial coordinate.

It is clearly seen from (28) that $\rho_{LOA}^{(2)}$ generally depends only on two ingredients, the correlation function $f(|\mathbf{r}_i - \mathbf{r}_j|)$ and the two-body density matrix in its mean-field approximation $\rho_{SD}^{(2)}$, (21). In the previous (25,26) we have already derived $\rho_{SD}^{(2)}$ in closed analytical form in terms of harmonic-oscillator single-particle wave functions. In order to find closed analytical expression for $\rho_{LOA}^{(2)}$, (28), we further assume that the correlation factor $f(\mathbf{r})$ is state-independent and has simple gaussian form:

$$f(\mathbf{r}) \equiv f(r) = \mathbf{1} - \mathbf{c} \exp(-\beta^2 r^2), \quad (29)$$

where the correlation parameter β controls the healing distance, while the parameter c accounts for the strength of

the SRC. Under these additional assumptions, performing explicitly the integrations entering (28), the diagonal part in the spin and isospin variables of $\rho_{LOA}^{(2)}$ transforms to pure algebraic expression:

$$\begin{aligned} \rho_{LOA}^{(2)}(\mathbf{r}_1, s_1, \tau_1; \mathbf{r}_2, s_2, \tau_2; \mathbf{r}_3, s_1, \tau_1; \mathbf{r}_4, s_2, \tau_2) \\ = \rho_{SD}^{(2)} + \rho_A^{(2)} + \rho_B^{(2)} + \rho_C^{(2)}, \end{aligned} \quad (30)$$

where the first term $\rho_{SD}^{(2)}$ is already defined by (25,26). The sum of this term $\rho_{SD}^{(2)}$ with the next one

$$\begin{aligned} \rho_A^{(2)} &= \frac{1}{2} \{ c^2 \exp[-(\mathbf{z}_1 - \mathbf{z}_2)^2 - (\mathbf{z}_3 - \mathbf{z}_4)^2] \\ &\quad - c \exp[-(\mathbf{z}_1 - \mathbf{z}_2)^2] - c \exp[-(\mathbf{z}_3 - \mathbf{z}_4)^2] \} \\ &\quad \times \{ \rho(\mathbf{r}_1, \mathbf{r}_3) \rho(\mathbf{r}_2, \mathbf{r}_4) - \delta_{\tau_1 \tau_2} \delta_{s_1 s_2} \rho(\mathbf{r}_1, \mathbf{r}_2) \rho(\mathbf{r}_3, \mathbf{r}_4) \}, \end{aligned} \quad (31)$$

where $\mathbf{z}_i = \beta \mathbf{r}_i$ is often referred to as a first order approximation to the Jastrow two-body density matrix [33]. The main disadvantage of this approximation is that it does not satisfy the normalization condition (6) and thus has restricted physical significance. The third term $\rho_B^{(2)}$ in (30) has the form:

$$\begin{aligned} \rho_B^{(2)} &= \frac{c^2}{2} \\ &\quad \cdot \left\{ 4 [\rho(\mathbf{r}_1, \mathbf{r}_3) \rho(\mathbf{r}_2, \mathbf{r}_4) \right. \\ &\quad - \delta_{\tau_1 \tau_2} \delta_{s_1 s_2} \rho(\mathbf{r}_1, \mathbf{r}_4) \rho(\mathbf{r}_2, \mathbf{r}_3)] (I_{13} + I_{24}) \\ &\quad - \rho(\mathbf{r}_1, \mathbf{r}_3) (I_{1324} + I_{2424}) - \rho(\mathbf{r}_2, \mathbf{r}_4) (I_{1313} + I_2) \\ &\quad + \delta_{\tau_1 \tau_2} \delta_{s_1 s_2} [\rho(\mathbf{r}_2, \mathbf{r}_3) (I_{1314} + I_{2414}) \\ &\quad + \rho(\mathbf{r}_1, \mathbf{r}_3) (I_{1324} + I_{2424})] \left. \right\} \\ &\quad - \frac{c}{2} \left\{ 4 [\rho(\mathbf{r}_1, \mathbf{r}_3) \rho(\mathbf{r}_2, \mathbf{r}_4) \right. \\ &\quad - \delta_{\tau_1 \tau_2} \delta_{s_1 s_2} \rho(\mathbf{r}_1, \mathbf{r}_4) \rho(\mathbf{r}_2, \mathbf{r}_3)] (I_1 + I_2 + I_3 + I_4) \\ &\quad - \rho(\mathbf{r}_1, \mathbf{r}_3) (I_{124} + I_{224} + I_{324} + I_{424}) \\ &\quad - \rho(\mathbf{r}_2, \mathbf{r}_4) (I_{113} + I_{213} + I_{331} + I_{413}) \\ &\quad + \delta_{\tau_1 \tau_2} \delta_{s_1 s_2} [\rho(\mathbf{r}_2, \mathbf{r}_3) (I_{114} + I_{214} + I_{314} + I_{414}) \\ &\quad - \rho(\mathbf{r}_1, \mathbf{r}_4) (I_{123} + I_{223} + I_{323} + I_{423})] \left. \right\}, \end{aligned} \quad (32)$$

while the last term $\rho_C^{(2)}$ reads:

$$\begin{aligned} \rho_C^{(2)} &= c \mathcal{M}(\mathbf{r}_1, s_1, \tau_1; \mathbf{r}_2, s_2, \tau_2; \mathbf{r}_3, s_1, \tau_1; \mathbf{r}_4, s_2, \tau_2; y) \\ &\quad - \frac{1}{2} c^2 \mathcal{M}(\mathbf{r}_1, s_1, \tau_1; \mathbf{r}_2, s_2, \tau_2; \mathbf{r}_3, s_1, \tau_1; \mathbf{r}_4, s_2, \tau_2; 2y), \end{aligned} \quad (33)$$

$$\begin{aligned} \mathcal{M} &= 4 [\rho(\mathbf{r}_1, \mathbf{r}_3) Y_{24} - \rho(\mathbf{r}_2, \mathbf{r}_4) Y_{13}] \\ &\quad - Y_{1324} + \rho(\mathbf{r}_1, \mathbf{r}_3) Z_{42} - \rho(\mathbf{r}_2, \mathbf{r}_4) Z_{13} \\ &\quad - \delta_{\tau_1 \tau_2} \delta_{s_1 s_2} \{ 4 [\rho(\mathbf{r}_1, \mathbf{r}_4) Y_{23} - \rho(\mathbf{r}_2, \mathbf{r}_3) Y_{14}] \\ &\quad - Y_{1423} - \rho(\mathbf{r}_2, \mathbf{r}_3) Z_{14} - \rho(\mathbf{r}_1, \mathbf{r}_4) Z_{23} \}. \end{aligned} \quad (34)$$

where the following products of exponential and polynomial factors depending on the scaled coordinates $\mathbf{x}_i = \alpha \mathbf{r}_i$ and the dimensionless parameter $y = \beta^2/\alpha^2$ are introduced:

$$\begin{aligned}
I_1 &= \exp\left[-\frac{yx_1^2}{1+y}\right] P_{I_1}(\mathbf{x}_1) \\
I_{12} &= \exp\left[-\frac{y(x_1^2 + x_2^2 + 2y(\mathbf{x}_1 - \mathbf{x}_2)^2)}{1+2y}\right] P_{I_2}(\mathbf{x}_1, \mathbf{x}_2) \\
I_{123} &= \frac{\alpha^3}{\pi^{3/2}} \exp\left[-\frac{x_2^2 + x_3^2 + y(2x_1^2 + x_2^2 + x_3^2)}{2(1+y)}\right] \\
&\quad \cdot P_{I_3}(\mathbf{x}_1, \mathbf{x}_2, \mathbf{x}_3) \\
I_{1234} &= \frac{\alpha^3}{\pi^{3/2}} \\
&\quad \exp\left[-\frac{x_3^2 + x_4^2 + 2y(x_1^2 + x_2^2) + 2y^2(\mathbf{x}_1 - \mathbf{x}_2)^2}{2(1+2y)}\right] \\
&\quad \cdot P_{I_4}(\mathbf{x}_1, \mathbf{x}_2, \mathbf{x}_3, \mathbf{x}_4) \tag{35}
\end{aligned}$$

and

$$\begin{aligned}
Y_{12} &= \frac{\alpha^3}{\pi^{3/2}} \exp\left[-\frac{x_1^2 + x_2^2}{2}\right] P_{Y_2}(\mathbf{x}_1, \mathbf{x}_2; y) \\
Z_{12} &= \frac{\alpha^3}{\pi^{3/2}} \exp\left[-\frac{x_1^2 + x_2^2}{2}\right] P_{Z_2}(\mathbf{x}_1, \mathbf{x}_2; y) \\
Y_{1234} &= \frac{\alpha^6}{\pi^3} \exp\left[-\frac{x_1^2 + x_2^2 + x_3^2 + x_4^2}{2}\right] \\
&\quad \cdot P_{Y_3}(\mathbf{x}_1, \mathbf{x}_2, \mathbf{x}_3, \mathbf{x}_4; y) \tag{36}
\end{aligned}$$

The two-body density matrix represented by (30-36) does not depend on the particular choice of the nucleus. All nuclear structure information is reflected by the polynomials $\{P_I, P_Y, P_Z\}$ entering (35,36). Their explicit form is given in the Appendix for ${}^4\text{He}$ and ${}^{16}\text{O}$ nuclei. As a result we end up with closed analytical algebraic expressions for the two-body density matrix involving three independent parameters, the harmonic oscillator length α and the correlations parameters c and β . Due to its gaussian-polynomial structure one can easily derive the Fourier transforms defining the associated two-body density matrix in the momentum space.

4 Local density and momentum pair distributions

Having derived the two-body density matrix in the coordinate space one is able to calculate all two-body nuclear characteristics in close analytical form. Changing the coordinates of two particles \mathbf{r}_1 and \mathbf{r}_2 in (30-36) to the center-of-mass $\mathbf{R} = (\mathbf{r}_1 + \mathbf{r}_2)/2$ and relative $\mathbf{s} = (\mathbf{r}_1 - \mathbf{r}_2)$ coordinates, one obtains the center-of-mass $\rho^{(2)}(\mathbf{R})$, (15), and relative $\rho^{(2)}(\mathbf{s})$, (16), pair local distributions. Using the dimensionless variables $R = \alpha|\mathbf{R}|$ and $s = \alpha|\mathbf{s}|$ they

have the following form:

$$\begin{aligned}
\rho^{(2)}(R) &= \mathcal{A} \exp\left[-\left(\sqrt{2}R\right)^2\right] \\
&\quad + \mathcal{B} \exp\left[-\frac{2(1+2y)}{2+3y}\left(\sqrt{2}R\right)^2\right] \\
&\quad + \mathcal{C} \exp\left[-\frac{1+4y}{1+3y}\left(\sqrt{2}R\right)^2\right], \tag{37}
\end{aligned}$$

$$\begin{aligned}
\rho^{(2)}(s) &= \mathcal{D} \exp\left[-\left(s/\sqrt{2}\right)^2\right] \\
&\quad + \mathcal{E} \exp\left[-\frac{2(1+2y)}{2+3y}\left(s/\sqrt{2}\right)^2\right] \\
&\quad + \mathcal{F} \exp\left[-\frac{1+4y}{1+3y}\left(s/\sqrt{2}\right)^2\right] \\
&\quad + \mathcal{G} \exp\left[-(1+4y)\left(s/\sqrt{2}\right)^2\right] \\
&\quad - \mathcal{H} \exp\left[-(1+2y)\left(s/\sqrt{2}\right)^2\right], \tag{38}
\end{aligned}$$

where

$$\begin{aligned}
\mathcal{A} &= \frac{\alpha^3}{\pi^{3/2}} [\eta_1(R) + 2c\eta_2(R, y) - c^2\eta_2(R, 2y)], \\
\mathcal{B} &= \frac{\alpha^3}{\pi^{3/2}} c\eta_3(R), \\
\mathcal{C} &= \frac{\alpha^3}{\pi^{3/2}} c^2\eta_4(R), \tag{39}
\end{aligned}$$

$$\begin{aligned}
\mathcal{D} &= \frac{\alpha^3}{\pi^{3/2}} [\mu_1(s) + 2c\mu_2(s; y) - c^2\mu_2(s; 2y)], \\
\mathcal{E} &= -\frac{\alpha^3}{\pi^{3/2}} 2c\mu_3(s; y), \\
\mathcal{F} &= \frac{\alpha^3}{\pi^{3/2}} c^2\mu_3(s; 2y) \\
\mathcal{G} &= \frac{\alpha^3}{\pi^{3/2}} c^2\mu_1(s), \\
\mathcal{H} &= -\frac{\alpha^3}{\pi^{3/2}} 2c\mu_1(s). \tag{40}
\end{aligned}$$

The center-of-mass $n^{(2)}(\mathbf{K})$, (17), and relative $n^{(2)}(\mathbf{k})$, (18), pair momentum distributions follow after performing Fourier transform of the center-of-mass $\rho^{(2)}(\mathbf{R}, \mathbf{R}')$ and relative $\rho^{(2)}(\mathbf{s}, \mathbf{s}')$ pair density matrices, respectively. Again, introducing $K = |\mathbf{K}|/\alpha$ and $k = |\mathbf{k}|/\alpha$ one obtains:

$$\begin{aligned}
n^{(2)}(\mathbf{K}) &= \mathcal{A}' \exp\left[-\left(\frac{K}{\sqrt{2}}\right)^2\right] \\
&\quad + \mathcal{B}' \exp\left[-\frac{1+2y}{2+5y}\left(\frac{K}{\sqrt{2}}\right)^2\right] \\
&\quad + \mathcal{C}' \exp\left[-\frac{1}{(1+y)}\left(\frac{K}{\sqrt{2}}\right)^2\right], \tag{41}
\end{aligned}$$

$$\begin{aligned}
n^{(2)}(\mathbf{k}) = & \mathcal{D}' \exp \left[- \left(\sqrt{2}k \right)^2 \right] \\
& + \mathcal{E}' \exp \left[- \frac{2(1+2y)}{2+5y} \left(\sqrt{2}k \right)^2 \right] \\
& + \mathcal{F}' \exp \left[- \frac{1}{1+y} \left(\sqrt{2}k \right)^2 \right] \\
& + \mathcal{G}' \exp \left[- \frac{1}{1+4y} \left(\sqrt{2}k \right)^2 \right] \\
& - \mathcal{H}' \exp \left[- \frac{1+2y}{1+4y} \left(\sqrt{2}k \right)^2 \right], \quad (42)
\end{aligned}$$

where

$$\begin{aligned}
\mathcal{A}' &= \frac{\sqrt{2}}{2\alpha^3 \pi^{3/2}} (\gamma_1(K) + 2c \gamma_2(K, y) - c^2 \gamma_2(K, 2y)), \\
\mathcal{B}' &= \frac{\sqrt{2}}{2\alpha^3 \pi^{3/2}} c \gamma_3(K), \quad \mathcal{C}' = \frac{\sqrt{2}}{2\alpha^3 \pi^{3/2}} c^2 \gamma_4(K), \quad (43) \\
\mathcal{D}' &= \frac{\sqrt{2}}{2\alpha^3 \pi^{3/2}} (\theta_1(k) + 2c \theta_2(k, y) - c^2 \theta_2(k, 2y)), \\
\mathcal{E}' &= \frac{\sqrt{2}}{2\alpha^3 \pi^{3/2}} c \theta_4(k), \quad \mathcal{F}' = \frac{\sqrt{2}}{2\alpha^3 \pi^{3/2}} c^2 \theta_6(k), \\
\mathcal{G}' &= \frac{\sqrt{2}}{2\alpha^3 \pi^{3/2}} c^2 \theta_5(k), \quad \mathcal{H}' = \frac{\sqrt{2}}{2\alpha^3 \pi^{3/2}} c \theta_3(k). \quad (44)
\end{aligned}$$

In the above expressions the exponential dependence is explicit while the expressions for the polynomial amplitudes $\{\eta_i\}$, $\{\mu_i\}$, $\{\gamma_i\}$ and $\{\theta_i\}$ are presented in the Appendix for ${}^4\text{He}$ and ${}^{16}\text{O}$ nuclei.

For completeness, we are giving also the local nuclear momentum distribution $n(k)$, (14), which is associated with the one-body density matrix. Its closed analytical form within the present model has already been derived in [18]:

$$\begin{aligned}
n(\mathbf{k}) = & \mathcal{A}'' \exp[-k^2] + \mathcal{B}'' \exp \left[- \frac{1}{1+2y} k^2 \right] \\
& - \mathcal{C}'' \exp \left[- \frac{1+2y}{1+3y} k^2 \right]. \quad (45)
\end{aligned}$$

and the polynomial expressions for the amplitudes \mathcal{A}'' , \mathcal{B}'' , \mathcal{C}'' can be found in [18]. Considering the gaussian factors one can realize a factor $\sqrt{2}$ which scales the momenta entering the three momentum distributions $n^{(2)}(\mathbf{K})$, $n(\mathbf{k})$ and $n^{(2)}(\mathbf{k})$.

5 Results and discussion

Next step in our study is to define the parameters of the problem, the oscillator parameter α and the parameters β and c related to the healing distance and the strength of the SRC, respectively. The rigorous procedure would be to apply the variational approach based on the one- and two-body density matrices defined so far by minimizing the total energy of the system with a realistic

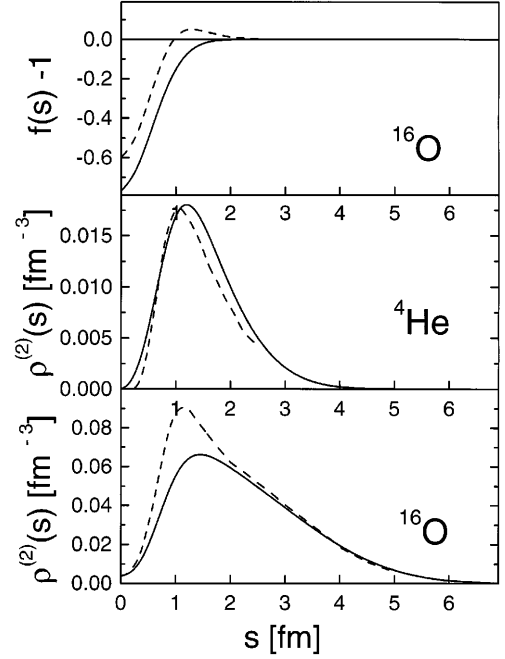


Fig. 1. Comparison of the present results (solid lines) with the Variational Monte-Carlo results for Argonne v_{14} potential [34] as obtained in [14], [13] (dashed lines). Top panel - comparison of the central correlation function. Next two panels - comparison of the relative pair density distributions normalized as $4\pi \int \rho^{(2)}(s) s^2 ds = 1$ for ${}^4\text{He}$ and ${}^{16}\text{O}$, respectively

NN -interaction with respect to the parameters α , β and c . As in our previous papers [18], however, we prefer to obtain the values of α and β phenomenologically by fitting the experimental elastic formfactor data using the analytical expression for the elastic formfactor following within the present model from (13). We should mention that effects like center-of-mass motion, meson exchange current effects, nucleon formfactors etc. are not taken into account in this kind of calculations. This fact together with the simple choice for the correlation factor and the single-particle wave functions are the actual restrictions of the present model considered.

The values of the parameter c for ${}^4\text{He}$ and ${}^{16}\text{O}$ are determined under the additional condition the relative pair density distribution $\rho^{(2)}(\mathbf{s})$, (38), to reproduce at $s = 0$ the associated value obtained within the Variational Monte-Carlo approach [13] and [14], respectively, while we simply put $c = 1$ for ${}^{40}\text{Ca}$ since there are no variational calculations for ${}^{40}\text{Ca}$. Thus, in the present numerical calculations we are using the following values of the parameters:

$$\begin{aligned}
\alpha &= 0.82 \text{ fm}^{-1}, \quad \beta = 1.23 \text{ fm}^{-1}, \quad c = 0.76 \quad \text{for } {}^4\text{He}, \\
\alpha &= 0.61 \text{ fm}^{-1}, \quad \beta = 1.30 \text{ fm}^{-1}, \quad c = 0.77 \quad \text{for } {}^{16}\text{O}, \\
\alpha &= 0.52 \text{ fm}^{-1}, \quad \beta = 1.21 \text{ fm}^{-1}, \quad c = 1.00 \quad \text{for } {}^{40}\text{Ca}. \quad (46)
\end{aligned}$$

At the beginning we are comparing in Fig. 1 some results from our crude but analytical model (the solid lines) with the results (dashed lines) emerging from the orders of magnitude more complicated Variational Monte-Carlo cal-

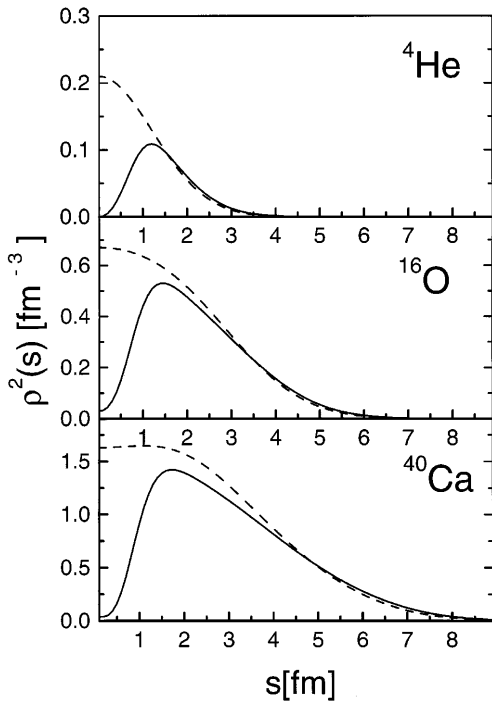


Fig. 2. Comparison between correlated ($c \neq 0$, solid lines) and uncorrelated ($c = 0$, dashed lines) results for the relative pair density distribution (38) normalized as $4\pi \int \rho^{(2)}(s)s^2 ds = 1$ for ${}^4\text{He}$, ${}^{16}\text{O}$ and ${}^{40}\text{Ca}$

culations [13], [14]. The top panel of Fig. 1 clearly demonstrates that our simple gaussian form for the correlation factor $f(r)$, (29), should be considered only as a first approximation to the actual shape of the realistic central correlation function. Nevertheless, the analytical results for the relative density pair distributions in ${}^4\text{He}$ and ${}^{16}\text{O}$ (two bottom panels in Fig. 1) show quite acceptable quantitative agreement with the Variational Monte-Carlo results. Despite of the simplicity of the model and the LOA used, the characteristic behavior of the realistic pair density is obviously reproduced. The small values of the relative pair distributions at $s = 0$ indicate the presence of significant SRC which in the Variational Monte-Carlo calculations are due to the repulsive core of the two-body interaction.

In Fig. 2a comparison is made between the correlated ($c \neq 0$, solid curves) and the uncorrelated ($c = 0$, dashed curves) results for the relative pair density distribution $\rho^{(2)}(\mathbf{s})$, (38), for ${}^4\text{He}$, ${}^{16}\text{O}$ and ${}^{40}\text{Ca}$. It is seen that due to the SRC the shape of the distributions changes significantly. The SRC lead to a deep hole in the correlated distributions near $s = 0$, while the uncorrelated distributions saturate at small distances to values which are significantly different from zero. Our calculations have shown that the SRC do not affect significantly the center-of-mass pair local distributions in the coordinate space.

The above examples show that despite of the simplicity of the model it is able to incorporate the SRC into the two-body quantities of interest. Therefore it may be con-

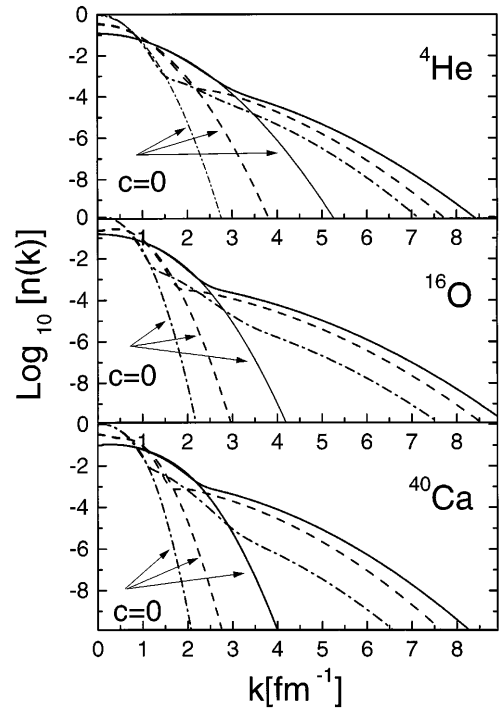


Fig. 3. Correlated ($c \neq 0$) and uncorrelated ($c = 0$) results for the center-of-mass $n^{(2)}(K)$ (solid curve) and relative $n^{(2)}(k)$ (dashed-dot curve) pair momentum distributions and for the nucleon momentum distribution $n(k)$ (dashed curve) for ${}^4\text{He}$ (top panel), ${}^{16}\text{O}$ (middle panel) and ${}^{40}\text{Ca}$ (bottom panel). All distributions are normalized to unity as e.g. $4\pi \int n(k)k^2 dk = 1$

sidered as a useful starting point in analyzing two-particle emission experiments.

From ($e, e'2N$) experiments one can expect important information about the effects of SRC on the pair local distributions in the momentum space. In Fig. 3 we present the center-of-mass (solid lines) $n^{(2)}(K)$, (41), and relative (dot-dashed lines) $n^{(2)}(k)$, (42), pair momentum distributions for ${}^4\text{He}$, ${}^{16}\text{O}$ and ${}^{40}\text{Ca}$. A comparison is also made between the correlated ($c \neq 0$) and uncorrelated ($c = 0$) results. For completeness, by dashed lines in Fig. 3, we also show the results for the local nuclear momentum distribution $n(k)$, (45), which is associated with the one-body density matrix.

From Fig. 3 is clearly seen that due to the SRC high momentum tails develop at large values of the momenta and this behavior is typical for all three kinds of momentum distributions considered. Comparing with the uncorrelated results one can see that the correlation effects start to dominate first for the relative pair momentum distribution $n^{(2)}(k)$. Then, at larger values of the momenta, the center-of-mass distribution $n^{(2)}(K)$ also develops a high momentum tail. The local nuclear momentum distribution $n(k)$ takes an intermediate position between both distributions $n^{(2)}(k)$ and $n^{(2)}(K)$. In the case of ${}^4\text{He}$ for example the SRC become important for mo-

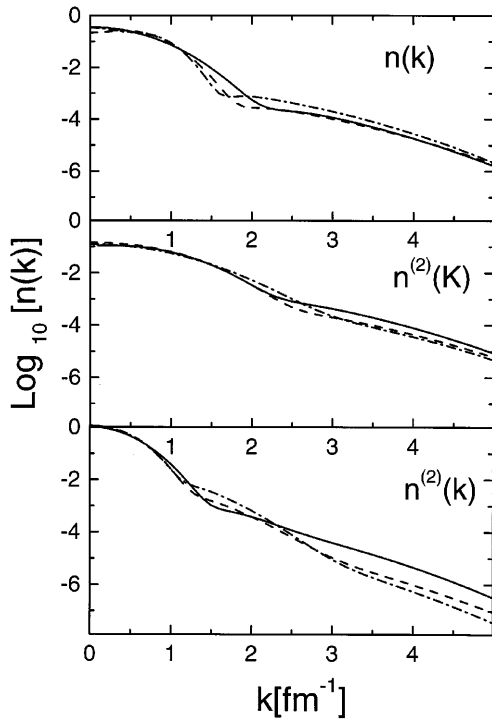


Fig. 4. Correlated momentum distributions from Fig. 3, $n(k)$ (top panel), $n^{(2)}(K)$ (middle panel) and $n^{(2)}(k)$ (bottom panel), but collected for all three nuclei ${}^4\text{He}$ (solid curve), ${}^{16}\text{O}$ (dashed curve) and ${}^{40}\text{Ca}$ (dashed-dot curve)

menta larger than 1.4, 2.1, 2.7 fm^{-1} , for the momentum distributions $n^{(2)}(k)$, $n(k)$ and $n^{(2)}(K)$, respectively. Similar values are valid also for nuclei ${}^{16}\text{O}$ and ${}^{40}\text{Ca}$. The reason for such behavior is obviously due to the scaling factor of $\sqrt{2}$ which has been observed in the analytical expressions for $n^{(2)}(K)$, (41), $n(k)$, (41) and $n^{(2)}(k)$, (42). Also, at large momenta both the correlated and uncorrelated momentum distributions obviously satisfy the inequality:

$$n^{(2)}(k) < n(k) < n^{(2)}(K) .$$

Of course, the comparison of the results given in Fig. 3 has to be done keeping in mind the different meaning of the arguments of the three types of momentum distributions considered..

Plotting together each of the nucleon momentum distributions $n^{(2)}(k)$, $n(k)$ and $n^{(2)}(K)$ for all nuclei ${}^4\text{He}$, ${}^{16}\text{O}$ and ${}^{40}\text{Ca}$, as it is done in Fig. 4, one can detect the interesting fact that in the high momentum region these distributions are almost universal in the sense that they do not significantly depend on the mass number A . This universal behavior of the local nucleon momentum distribution $n(k)$ has been observed earlier (see e.g. [14,18,22]). Obviously similar tendency exists also for the relative and center-of-mass pair momentum distributions.

6 Conclusions

In this paper we have derived closed analytical expressions for the two-body density matrix and associated two-body nuclear characteristics within the LOA to the Jastrow correlation method for the closed $s - d$ shell nuclei ${}^4\text{He}$, ${}^{16}\text{O}$ and ${}^{40}\text{Ca}$ under two simplifying assumptions: harmonic-oscillator single-particle wave functions entering the Slater determinant and a state-independent gaussian-like correlation function. The comparison with more realistic results emerging from Variational Monte-Carlo calculations has shown the usefulness of the expressions derived. They can be applied as a starting tool in analyzing two-particle emission experiments where important information about the effects of SRC on the two-body nuclear characteristics is expected. In particular, it has been shown that the SRC effects start to dominate in the high-momentum region of the relative $n^{(2)}(k)$, local $n(k)$ and center-of-mass $n^{(2)}(K)$ momentum distributions at different momentum values which are proportional to a factor of $\sqrt{2}$ and are almost independent on the nucleus considered. An universal asymptotic behavior of the relative and center-of-mass pair momentum distributions (normalized to unity) is indicated similar to the well known high-momentum tail of the nucleon momentum distribution $n(k)$.

As a first approximation, the simplicity of the results can help us to concentrate our attention towards the complicated questions arising from the involved physical interpretation and the mechanism of the two-particle emission processes in nuclei.

One of the authors (S.S.D) is grateful to Dr. P.E. Hodgson and the Royal Society for the warm hospitality and financial support at the Astrophysics and Nuclear Physics Laboratory of the Oxford University. This work is supported in part by the Contract $\Phi - 809$ with the Bulgarian National Science Foundation.

Appendix

A.1 Polynomials entering the two-body density matrix

The expressions for $\{P\}$ in (35,36) which determine the two-body density matrix are:

A.1.1 Nucleus ${}^4\text{He}$

$$P_{I_1} = P_{I_2} = (1 + 2y)^{-3/2}$$

$$P_{I_3} = P_{I_4} = (1 + y)^{-3/2}$$

$$P_{Y_2}(y) = P_{Z_2}(y) = P_{Y_3}(y) = (1 + 2y)^{-3/2}$$

A.1.2 Nucleus ^{16}O

$$\begin{aligned}
P_{I_1}(\mathbf{x}) &= \frac{1}{(1+y)^{7/2}} [4 + 5y + y^2 (1 + 2x^2)] \\
P_{I_2}(\mathbf{x}_1, \mathbf{x}_2) &= \frac{2}{(1+2y)^{7/2}} \\
&\cdot [2 + 5y + y^2 (2 + x_1^2 + x_2^2 + 2x_{12})] \\
P_{I_3}(\mathbf{x}_1, \mathbf{x}_2, \mathbf{x}_3) &= \frac{1}{(1+y)^{7/2}} [1 + 2x_{23} + 2y \\
&\cdot (1 + x_{12} + x_{13} + x_{23}) \\
&+ y^2 (1 + 2x_{12} + 2x_{13} + 4x_{12}x_{13})] \\
P_{I_4}(\mathbf{x}_1, \mathbf{x}_2, \mathbf{x}_3, \mathbf{x}_4) &= \frac{1}{(1+2y)^{7/2}} [1 + 2x_{34} + 2y \\
&\cdot (2 + x_{13} + x_{14} + x_{23} + x_{24} + 2x_{34}) \\
&+ 4y^2 (x_{13} + x_{14} + x_{23} + x_{24} + x_{23} + x_{13}x_{14} \\
&+ x_{14}x_{23} + x_{13}x_{24}x_{24})]
\end{aligned}$$

$$\begin{aligned}
P_{Y_2}(\mathbf{x}_1, \mathbf{x}_2; y) &= \frac{1}{(1+2y)^{7/2}} \\
&\cdot [4 + 8x_{12} + y(13 + 18x_{12}) + y^2(10 + 14x_{12})] \\
P_{Z_2}(\mathbf{x}_1, \mathbf{x}_2; y) &= \frac{1}{(1+2y)^{7/2}} \\
&\cdot [1 + 2x_{12} + y(7 + 6x_{12}) + y^2(10 + 14x_{12})] \\
P_{Y_3}(\mathbf{x}_1, \mathbf{x}_2, \mathbf{x}_3, \mathbf{x}_4; y) &= \frac{1}{(1+2y)^{7/2}} \\
&\cdot [1 + 2x_{12} + 2x_{34} + 4x_{12}x_{34} + \\
&+ 2y(2 + 3x_{12} + x_{13} + x_{14} + x_{23} + x_{24} + 3x_{34} + 4x_{12}x_{34}) \\
&+ 4y^2(1 + x_{12} + x_{13} + x_{14} + x_{23} + x_{24} + x_{34} + x_{14}x_{23} \\
&+ x_{13}x_{24} + x_{12}x_{34})]
\end{aligned}$$

A.1.3 Nucleus ^{40}Ca

The expressions for ^{40}Ca have similar structure but are up to 4-th order with respect to x_{ij} , thus being too long to be presented here. They can be obtained in the form of user friendly files for Mathematica 3.0 upon request.

A.2 Polynomials entering local density pair distributions

The expressions for $\{\eta_i\}$, $\{\mu_i\}$, $\{\gamma_i\}$ and $\{\theta_i\}$, which determine the two-body density and momentum distributions (37-42) are:

A.2.1 Nucleus 4He

$$\begin{aligned}
\eta_1(R) &= 12\sqrt{2} & \eta_2(R; y) &= -\frac{4\sqrt{2}}{(1+2y)^{3/2}} \\
\eta_3(R) &= \frac{32}{(2+3y)^{3/2}} & \eta_4(R) &= -\frac{4\sqrt{2}}{(1+3y)^{3/2}} \\
\mu_1(s) &= \frac{3}{\sqrt{2}} & \mu_2(s; y) &= \frac{15}{\sqrt{2}(1+2y)^{3/2}} \\
\mu_3(s; y) &= \frac{24}{(2+3y)^{3/2}} \\
\gamma_1(K) &= \frac{1}{2} & \gamma_2(K, y) &= \frac{2}{(1+2y)^{3/2}} \\
\gamma_3(K) &= -\frac{8\sqrt{2}}{(2+5y)^{3/2}} & \gamma_4(K) &= \frac{2}{(1+y)^{3/2}(1+4y)^{3/2}} \\
\theta_1(k) &= 4 & \theta_2(k; y) &= \frac{20}{(1+2y)^{3/2}} \\
\theta_3(k) &= -\frac{8}{(1+4y)^{3/2}} \\
\theta_4(k) &= -\frac{64\sqrt{2}}{(2+5y)^{3/2}} & \theta_5(k) &= \frac{4}{(1+4y)^3} \\
\theta_6(k) &= \frac{16}{(1+y)^{3/2}(1+4y)^{3/2}}
\end{aligned}$$

A.2.2 Nucleus ^{16}O

$$\begin{aligned}
\eta_1(R) &= 2\sqrt{2} (117 + 104R^2 + 48R^4) \\
\eta_2(R; y) &= \frac{\sqrt{2}}{(1+2y)^{7/2}} [48R^4 (28 + 60y + 35y^2) \\
&+ 8R^2 (364 + 848y + 555y^2) \\
&+ 3(1092 + 2780y + 1837y^2)] \\
\eta_3(R) &= -\frac{128}{(2+3y)^{15/2}} [1536R^6 y^2 (1 + 3y + 2y^2)^2 \\
&+ 192R^4 (28 + 224y + 749y^2) \\
&+ 1352y^3 + 1419y^4 + 843y^5 + 225y^6) \\
&+ 8R^2 (2 + 3y)^2 (364 + 1762y + 3489y^2) \\
&+ 3105y^3 + 990y^4) \\
&+ 9(2 + 3y)^3 (182 + 563y + 588y^2 + 212y^3)] \\
\eta_4(R) &= \frac{4\sqrt{2}}{(1+3y)^{15/2}} [384R^6 y^2 (1 + 6y + 8y^2)^2 \\
&+ 48R^4 (7 + 112y + 749y^2 + 2704y^3) \\
&+ 5676y^4 + 6744y^5 + 3600y^6) \\
&+ 8R^2 (1 + 3y)^2 (91 + 881y + 3489y^2) \\
&+ 6210y^3 + 3960y^4) \\
&+ 9(1 + 3y)^3 (91 + 563y + 1176y^2 + 848y^3)]
\end{aligned}$$

$$\begin{aligned}
\mu_1(s) &= \frac{1}{4\sqrt{2}} (93 + 34s^2 + 3s^4) & \theta_1(k) &= \frac{1}{60} (117 + 104k^2 + 48k^4) \\
\mu_2(s; y) &= \frac{1}{4\sqrt{2}(1+2y)^{7/2}} [2697 + 6540y + 4047y^2 & \theta_2(k; y) &= \frac{1}{60(1+2y)^{7/2}} [48k^4(29 + 64y + 39y^2) \\
&+ 2s^2(493 + 1214y + 831y^2) & &+ 8k^2(493 + 1202y + 807y^2) \\
&+ 3s^4(29 + 64y + 39y^2)] & &+ 3(899 + 2204y + 1397y^2)] \\
\mu_3(s; y) &= \frac{8}{(2+3y)^{15/2}} [3(2+3y)^3(434 + 1245y & \theta_3(k) &= -\frac{1}{30(1+4y)^{7/2}} [48k^4 + 8k^2(17 + 80y + 24y^2) \\
&+ 1158y^2 + 348y^3) + 2s^2(2+3y)^2 & &+ 3(31 + 224y + 400y^2)] \\
&\cdot (476 + 2370y + 4713y^2 + 4215y^3 + 1386y^4) & \theta_4(k) &= \frac{16\sqrt{2}}{15(2+5y)^{5/2}} \\
&+ 12s^4(28 + 232y + 813y^2 + 1554y^3) & &\cdot [1536k^6y^2(1+2y)^2(1+4y+3y^2) \\
&+ 1733y^4 + 1083y^5 + 297y^6) & &- 3(2+5y)^3(434 + 2571y + 4800y^2 + 2870y^3) \\
&+ 24s^6y^2(1+3y+2y^2)^2] & &- 8k^2(2+5y)^2(476 + 3774y + 11043y^2 \\
& & &+ 14075y^3 + 6780y^4) - 192k^4(28 + 344y \\
& & &+ 1697y^2 + 4268y^3 + 5691y^4 + 3727y^5 + 905y^6)] \\
\gamma_1(K) &= \frac{1}{480} (117 + 26K^2 + 3K^4) & \theta_5(k) &= \frac{1}{60(1+4y)^7} [48k^4 + 8k^2(17 + 160y + 368y^2) \\
& & &+ 3(1+4y)^2(31 + 200y + 496y^2)] \\
\gamma_2(K; y) &= \frac{1}{480(1+2y)^{7/2}} [3K^4(28 + 60y + 35y^2) & \theta_6(k) &= \frac{1}{15(1+y)^{11/2}(1+4y)^{7/2}} [48k^4(7 + 46y + 72y^2) \\
&+ 2K^2(364 + 872y + 603y^2) & &+ 8k^2(119 + 935y + 2862y^2 + 3890y^3 + 1844y^4) \\
&+ 3(1092 + 2732y + 1741y^2)] & &+ 3(1+y)^2(217 + 1486y + 4236y^2 + 5944y^3 \\
& & &+ 3472y^4)] \\
\gamma_3(K) &= \frac{2\sqrt{2}}{15(2+5y)^{15/2}} & & \\
&\cdot [24K^6y^2(1+2y)^2(1+4y+3y^2) & & \\
&- 12K^4(28 + 344y + 1705y^2 + 4340y^3 & & \\
&+ 5933y^4 + 4087y^5 + 1105y^6) & & \\
&- 2K^2(2+5y)^2(364 + 2870y + 8263y^2 & & \\
&+ 10185y^3 + 4680y^4) - 3(2+5y)^3 & & \\
&\cdot (546 + 3251y + 6160y^2 + 3770y^3)] & & \\
\gamma_4(K) &= \frac{1}{120(1+y)^{11/2}(1+4y)^{7/2}} & & \\
&\cdot [3K^4(7 + 46y + 72y^2) + 2K^2(91 + 707y & & \\
&+ 2250y^2 + 3238y^3 + 1604y^4) & & \\
&+ 3(1+y)^2(273 + 1886y + 5060y^2 & & \\
&+ 6424y^3 + 3472y^4)] & &
\end{aligned}$$

A.2.3 Nucleus ^{40}Ca

Again, the expressions for ^{40}Ca have similar structure but are too long to be presented here. They can be obtained in the form of user friendly files for Mathematica 3.0 upon request.

References

1. C. Guisti and F. D. Pacati, Nucl. Phys. A **641**, 297 (1998)
2. J. Ryckebusch, Phys. Lett. B **383**, 1 (1996)
3. J. Ryckebusch, V. Van der Sluys, K. Heyde, H. Holvoet, W. Van Nespren, M. Waroquier, M. Vanderhaeghen, Nucl. Phys. A **624**, 581 (1997)
4. C. Guisti and F. D. Pacati, Nucl. Phys. A **615**, 373 (1997)
5. C. J. Onderwater et al., Phys. Rev. Lett. **78**, 4893 (1997)
6. C. Guisti, F. D. Pacati, K. Allaart, W. J. W. Geurts, W. H. Dickhoff and H. Mütter, Phys. Rev. C **57**, 1691 (1998)

7. S. Boffi, C. Guisti, F. Pacati and M. Radici, *Electromagnetic Response of Atomic Nuclei*, Oxford Studies in Nuclear Physics (Clarendon Press, Oxford, 1996).
8. W. J. W. Geurts, K. Allaart, W. H. Dickhoff and H. Mütter, Phys. Rev. C **54**, 1144 (1996).
9. C. Guisti and F. D. Pacati, Nucl. Phys. A **535**, 573 (1991)
10. G. Orlandini and L. Sarra, Invited talk at the Second Workshop on "Electromagnetically Induced Two-Nucleon Emission", Belgium, May 17–20, 1995
11. E. Mavrommatis, M. Petraki and J. W. Clark, Phys. Rev. C **51**, 1849 (1995)
12. R. Schiavilla, V.R. Pandharipande and R.B. Wiringa, Nucl. Phys. A **449**, 219 (1986)
13. L. Carlson, Phys. Rev. C **38**, 1879 (1988)
14. S.C. Pieper, R.B. Wiringa and V.R. Pandharipande, Phys. Rev. C **46**, 1741 (1992)
15. B.C. Pudliner, V.R. Pandharipande, S.C. Pieper and R.B. Wiringa, Phys. Rev. C **56**, 1720 (1997)
16. D. Van Neck, M. Waroquier and K. Heyde, Phys. Lett. B **314**, 255 (1993)
17. M. V. Stoitsov, S. S. Dimitrova and A. N. Antonov, Phys. Rev. C **53**, 1254 (1996)
18. M. V. Stoitsov, A. N. Antonov and S. S. Dimitrova, Phys. Rev. C **47**, R455 (1993); Phys. Rev. C **48**, 74 (1993); Z. Phys. A **345**, 359 (1993)
19. P.-O. Löwdin, Phys. Rev. **97**, 1474 (1955)
20. D. S. Lewart, V. R. Pandharipande and S. C. Pieper, Phys. Rev. B **37**, 4950 (1988)
21. C. Mahaux and R. Sartor, Adv. Nucl. Phys. **20**, 1 (1991)
22. A. N. Antonov, P. E. Hodgson and I. Zh. Petkov, *Nucleon Momentum and Density Distributions in Nuclei*, (Clarendon Press, Oxford, 1988); *Nucleon Correlations in Nuclei* (Springer-Verlag, Berlin-Heidelberg-New York, 1993)
23. S.S. Dimitrova, M.K. Gaidarov, A.N. Antonov, M.V. Stoitsov, P.E. Hodgson, V.K. Lukyanov, E.V. Zemlyanaya, G.Z. Krumova, Journal of Physics G **23**, 1685 (1997)
24. D. Van Neck, L. Van Daele, Y. Dewulf, and M. Waroquier, Phys. Rev. C **56**, 1398 (1997)
25. J.E. Amaro, A.M. Lallena, G. Co', and A. Fabrocini, Phys. Rev. C **57**, 3473 (1998)
26. H. Mütter, A. Polls, and W.H. Dickhoff, Phys. Rev. C **51**, 3040 (1995)
27. M.K. Gaidarov, K.A. Pavlova, S.S. Dimitrova, M.V. Stoitsov, A.N. Antonov, D. Van Neck and H. Mütter, nucl-th/9904022; Phys. Rev. C **60**, 024312 (1999)
28. A.N. Antonov, S.S. Dimitrova, M.V. Stoitsov, D. Van Neck and P. Jeleva, **Phys. Rev. C** **59**, 722 (1999)
29. R. Jastrow, Phys. Rev. **98**, 1479 (1955)
30. M. Gaudin, J. Gillespie, G. Ripka, Nucl. Phys. A **176**, 237 (1971)
31. O. Bohigas, S. Stringari, Phys. Lett. B **98**, 9 (1982)
32. M. Dal Rí, S. Stringari, O. Bohigas, Nucl. Phys. A **376**, 81 (1982)
33. G. Ripka, Phys. Rep. **56**, 1 (1979)
34. R.B. Wiringa, R.A. Smith and T.L. Ainsworth, Phys. Rev. C **29**, 1207 (1984)